PqsL uses reduced flavin to produce 2-hydroxylaminobenzoylacetate, a preferred PqsBC substrate in alkyl quinolone biosynthesis in *Pseudomonas aeruginosa*

Received for publication, November 3, 2017, and in revised form, April 6, 2018 Published, Papers in Press, April 18, 2018, DOI 10.1074/jbc.RA117.000789

Steffen Lorenz Drees[‡1], **Simon Ernst**[‡], **Benny Danilo Belviso**[§], **Nina Jagmann**[‡], **Ulrich Hennecke**[¶], and **Susanne Fetzner**[‡2]

From the [‡]*Institute for Molecular Microbiology and Biotechnology and* [¶]*Organic Chemistry Institute, University of Münster, D-48149 Münster, Germany and the* [§]*Institute of Crystallography, Consiglio Nazionale delle Ricerche, 70126 Bari, Italy*

Edited by F. Peter Guengerich

Alkyl hydroxyquinoline *N*-oxides (AQNOs) are antibiotic compounds produced by the opportunistic bacterial pathogen *Pseudomonas aeruginosa*. They are products of the alkyl quinolone (AQ) biosynthetic pathway, which also generates the quorum-sensing molecules 2-heptyl-4(1*H*)-quinolone (HHQ) and 2-heptyl-3-hydroxy-4(1*H*)-quinolone (PQS). Although the enzymatic synthesis of HHQ and PQS had been elucidated, the route by which AQNOs are synthesized remained elusive. Here, we report on PqsL, the key enzyme for AQNO production, which structurally resembles class A flavoprotein monooxygenases such as *p*-hydroxybenzoate 3-hydroxylase (pHBH) and 3-hydroxybenzoate 6-hydroxylase. However, we found that unlike related enzymes, PqsL hydroxylates a primary aromatic amine group, and it does not use NAD(P)H as cosubstrate, but unexpectedly required reduced flavin as electron donor. We also observed that PqsL is active toward 2-aminobenzoylacetate (2-ABA), the central intermediate of the AQ pathway, and forms the unstable compound 2-hydroxylaminobenzoylacetate, which was preferred over 2-ABA as substrate of the downstream enzyme PqsBC. *In vitro* reconstitution of the PqsL/PqsBC reaction was feasible by using the FAD reductase HpaC, and we noted that the AQ:AQNO ratio is increased in an *hpaC*-deletion mutant of *P. aeruginosa* PAO1 compared with the ratio in the WT strain. A structural comparison with pHBH, the model enzyme of class A flavoprotein monooxygenases, revealed that structural features associated with NAD(P)H binding are missing in PqsL. Our study completes the AQNO biosynthetic pathway in *P. aeruginosa*, indicating that PqsL produces the unstable product 2-hydroxylaminobenzoylacetate from 2-ABA and depends on free reduced flavin as electron donor instead of NAD(P)H.

This work was supported by Deutsche Forschungsgemeinschaft Grants FE 383/23-1 and FE 383/23-2 (to S. F.) and HE 6020/3-1 (to U. H.). The authors declare that they have no conflicts of interest with the contents of this article.

The atomic coordinates and structure factors (code 6FHO) have been deposited in the Protein Data Bank (http://wwpdb.org/).

[1] Recipient of a research fellowship from the Heinrich-Hertz-Stiftung. To whom correspondence may be addressed. Tel.: 49-251-8339835; Fax: 49-251-8338388; E-mail: s.drees@uni-muenster.de.

[2] To whom correspondence may be addressed. Tel.: 49-251-8339824; Fax: 49-251-8338388; E-mail: fetzner@uni-muenster.de.

The opportunistic pathogen *Pseudomonas aeruginosa* produces numerous 2-alkyl-4-hydroxyquinoline-type secondary metabolites (AQ),[3] which differ in the length and degree of saturation of the alkyl side chain, the substituent (–H or –OH) at the C3 position, and the oxidation state of the quinoline nitrogen (1). AQs exert various and often multiple biological activities and significantly contribute to virulence as well as competitiveness within bacterial communities (2). Although 2-heptyl-3-hydroxy-4(1*H*)-quinolone (*Pseudomonas* quinolone signal, PQS) and its immediate biosynthetic precursor 2-heptyl-4(1*H*)-quinolone (HHQ) mainly serve as quorum-sensing signals, contributing to the control of virulence gene expression (3, 4), 2-heptyl-4-hydroxyquinoline-*N*-oxide (HQNO) acts as a toxin against both microorganisms and eukaryotic cells. HQNO binds to the quinone reduction (Q_i) site of the respiratory cytochrome bc_1 complex (5), and it also inhibits the quinol oxidase activity of cytochrome bo_3 and *bd* (6, 7) and quinone reduction by type II NADH-quinone oxidoreductase (8). Exposure of *Staphylococcus aureus* to HQNO selects for small-colony variants, which are known for long persistence during chronic infections. HQNO, together with siderophores, plays a key role in reduction of *S. aureus* viability by *P. aeruginosa* (9). However, HQNO also causes self-poisoning of *P. aeruginosa*, finally leading to autolysis, which potentially is advantageous to the bacterial population, promoting biofilm formation by the surviving cells (10). HQNO and its nonyl congener are among the most abundant AQ compounds produced by *P. aeruginosa* (1, 11, 12).

2-Alkyl-4-hydroxyquinoline-*N*-oxide (AQNO) biosynthesis involves the enzymes encoded by the *pqsABCDE* operon (PA0996–PA1000), which mediate 2-alkyl-4-hydroxyquinoline biosynthesis from anthranilic acid and activated fatty acids (Fig. 1), and additionally requires PqsL, a putative flavin-dependent monooxygenase encoded by a presumably monocistronic

[3] The abbreviations used are: AQ, 2-alkyl-hydroxyquinoline; 2-ABA, 2-aminobenzoylacetate; 2-HABA, 2-(hydroxylamino)benzoylacetate; 2-NBA, 2-nitrobenzoylacetate; AQNO, 2-alkyl-4-hydroxyquinoline-*N*-oxide; DHQ, 2,4-dihydroxyquinoline; HHQ, 2-heptyl-4(1*H*)quinolone; HQNO, 2-heptyl-4-hydroxyquinoline-*N*-oxide; pHBH *p*-hydroxybenzoate-3-monooxygenase; pHPA, *p*-hydroxyphenylacetate; PQS, *Pseudomonas* quinolone signal, 2-heptyl-3-hydroxy-4(1*H*)-quinolone; PDB, Protein Data Bank; fw, forward; rev, reverse; SOE-PCR, second overlapping PCR.

gene (PA4190) (1, 13). Because *P. aeruginosa* supplemented with deuterated HHQ failed to produce deuterated HQNO, the *N*-oxides most probably are not synthesized by hydroxylation of 2-alkyl-4-hydroxyquinolines (14). However, feeding of 2-aminobenzoylacetate (2-ABA) (Fig. 1) to a *pqsA*$^{-}$/*pqsH*$^{-}$ mutant (which is unable to produce HHQ and to convert exogenously supplied HHQ to PQS) resulted in formation of HQNO along with HHQ (15), suggesting that AQNO biosynthesis branches off from 2-ABA or an immediate downstream intermediate.

The crystal structure of the PqsL protein (PDB code 2X3N) was determined by Oke *et al.* (16) within the frame of a high-throughput crystallization screen, but the functional properties of the protein have not been investigated. PqsL is a member of the UbiH family (Prosite/ExPASy family PS01304 (17)). Structural analyses suggested similarity to class A flavoprotein monooxygenases. The prototype enzyme of this class is *p*-hydroxybenzoate-3-monooxygenase (pHBH) (18). Class A enzymes depend on NADPH or NADH, contain a tightly bound FAD cofactor, are encoded by a single gene, and feature a GSH reductase fold comprising one dinucleotide-binding domain (Rossmann fold). The oxygenating flavin species, the C(4a)-hydroperoxyflavin, performs an electrophilic attack on the substrate, which for the majority of the known members of this class is an aromatic compound containing a hydroxyl or amino group. Many members of this flavoprotein monooxygenase class are involved in the microbial degradation of aromatic compounds. However, several halogenases taking part in biosynthetic pathways of antibiotics also show structural resemblance to pHBH (19). They require reduced FAD, produced by a reductase, as well as molecular oxygen for catalysis and have been classified within the class F flavoprotein monooxygenases (18). Class F monooxygenases were suggested to have a class A-like ancestor (20).

In this study, we complete the HQNO biosynthetic pathway by characterizing the PqsL reaction, which produces the unstable product 2-hydroxylaminobenzoylacetate (2-HABA) from 2-ABA, and unexpectedly depends on free reduced flavin as electron donor in lieu of NAD(P)H. By re-analyzing the available crystallographic data and comparing them with the pHBH structure, we found indications that key residues involved in NAD(P)H recognition are lacking in PqsL, which supports our biochemical data. We also identified PqsBC as the enzyme that catalyzes the condensation of 2-HABA with activated octanoate to produce HQNO. We propose that the preference of PqsBC for 2-HABA over 2-ABA prevents accumulation of the highly reactive *N*-aryl hydroxylamine compound.

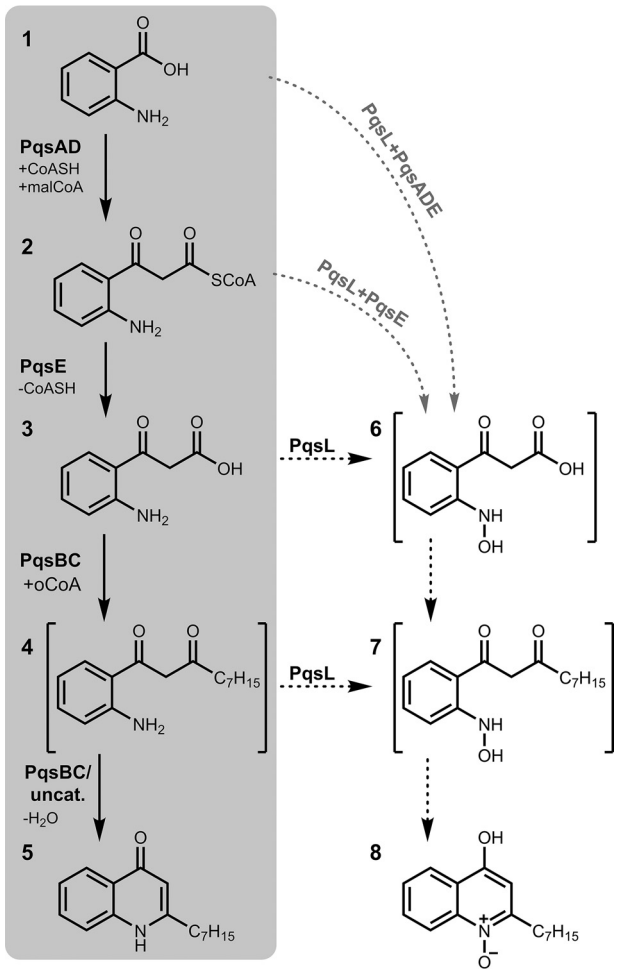

Figure 1. Biosynthesis of alkyl quinolones in *P. aeruginosa* (*shaded box*) (15, 66, 79, 80) and possible reactions for HQNO synthesis. It was demonstrated before that HHQ (*#5*) is not the precursor of HQNO (*#8*) and that feeding 2-ABA (*#3*) to a 2-ABA-nonproducing mutant yields HQNO (14, 15). Therefore, two possible substrates can be hypothesized for PqsL, 2-aminobenzoylacetate (*#3*) or the hypothetical 1-(2-aminophenyl)decane-1,3-dione (*#4*, initial, short-lived product of the PqsBC-catalyzed condensation reaction). Possible reaction routes are illustrated by *dashed arrows*. However, alternative or additional reactions involving anthranilate/anthraniloyl-CoA (*#1*) or 2-aminobenzoylacetyl-CoA (*#2*, short-lived) as PqsL substrates cannot be excluded entirely, as indicated by *gray dashed arrows*. *malCoA,* malonyl-CoA; *oCoA,* octanoyl-CoA.

Results and discussion

Purification of PqsL

PqsL, the key enzyme for biosynthesis of HQNO, catalyzes the *N*-oxidation of a biosynthetic precursor molecule other than HHQ (14). Despite long-standing evidence for an alternative biosynthetic route, the substrate of PqsL was unknown, and its reaction had not been characterized so far. We purified PqsL as a fusion protein with an N-terminal His- or Strep-tag as well as a C-terminal His-tag to identify its most active form. Cofactor content analysis by regression of UV/visible spectra showed that only between 75 and 82% of the PqsL protein carried an FAD cofactor, irrespective of the type and position of the affinity tag. However, FAD occupancy could be improved to over 95% by incubating the protein with equimolar concentrations of FAD and subsequent size-exclusion chromatography. The protein was stable for 24 h at 4 °C. The purified recombinant proteins did not show any differences in activity or substrate selectivity. Because the N-terminally His-tagged protein was easiest to produce at high yields (>20 mg liter^{-1} of culture), it was used for the experiments described below.

In vitro activity of PqsL toward 2-ABA with chemically reduced FAD

Initially, we tested NADH or NADPH oxidation by PqsL in the presence of 2-ABA and other available intermediates of the AQ pathway as possible substrates (see Fig. 1). Despite trying an

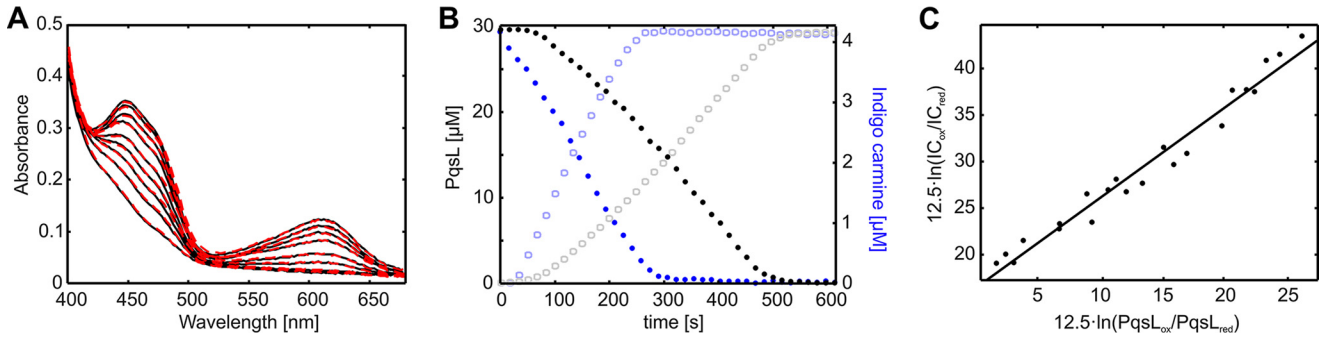

Figure 2. Midpoint potential of PqsL-bound FAD. *A,* representative spectra of the reduction of a PqsL/indigo carmine solution (PqsL and indigo carmine spectra shown in Fig. S1) *Black lines* indicate measured data, and *red lines* are composite spectra from least squares fitting. *B*, reduction of PqsL and indigo carmine as calculated from the fitting (one representative experiment). *Solid points* reflect oxidized species; *open points* indicate reduced species concentrations (PqsL, *black*; indigo carmine, *blue*). *C,* Nernst plot comprising data collected in three independent experiments.

array of reaction conditions, substrate-stimulated NAD(P)H oxidation was not detected. Interestingly, in contrast to homologous group A flavoprotein monooxygenases such as pHBH, flavin reduction by NADH or NADPH under anoxic conditions was not observed, irrespective of the presence of potential substrates. In pHBH, absence of the substrate pHB was reported to diminish the FAD reduction rate by a factor of 10^5; nevertheless, FAD reduction was measurable within minutes (21). Thus, even if PqsL used another organic substrate (such as the hypothetical 1-(2-aminophenyl)decane-1,3-dione, see Fig. 1), FAD reduction by the reducing co-substrate would have been expected to occur. Therefore, we attempted to identify the organic substrate of PqsL in a co-substrate–independent approach. First, the PqsL-bound FAD was pre-reduced under anoxic conditions with sodium dithionite until the yellow color was almost bleached out. Then, we performed an assay combining PqsL with the PqsBC reaction in which the expected reaction products HHQ and/or HQNO were quantified by HPLC. When dithionite-reduced PqsL was mixed with an excess of 2-ABA and added to air-saturated buffer containing 1 μM PqsBC and an excess of octanoyl-CoA, HQNO, produced by a single PqsL turnover, was observed besides HHQ. Without pre-reduction of the flavin cofactor of PqsL, HQNO was not detected. We hence concluded that, once FAD is reduced, 2-ABA or a hypothetical intermediate formed by PqsBC is the substrate oxidized by PqsL.

Remarkably, the addition of anoxically reduced free FAD (assay concentration between 20 and 200 μM, ~90% total $FADH_2$ content) to a mixture of 10 μM PqsL, 1 μM PqsBC, and 50 μM substrates 2-ABA and octanoyl-CoA, instantaneously mixed in an air-saturated buffer, also led to formation of HQNO (<10 μM), indicating that PqsL is able to receive electrons from reduced FAD. Alternatively, PqsL might exchange its internal FAD cofactor for $FADH_2$; however, because the reaction could be supported by reduced FMN as well (albeit with lower efficiency), we believe that a cofactor exchange is rather unlikely.

Redox potential of PqsL is sufficiently positive for direct reduction by free flavin

To investigate the electrochemical properties of the PqsL-internal flavin, we determined its two-electron midpoint potential. The potential of free FAD (−210 mV) (22–24) can be severely affected by protein binding. Based on available data, it can be generalized that this potential seems to shift to slightly more positive values of about −180 to −200 mV in class A monooxygenases (22, 25, 26). Thermodynamically, this small gap in potential would suffice to facilitate electron transfer from free $FADH_2/FADH^-$ to protein-bound FAD. In light of the peculiarities of PqsL regarding co-substrate utilization, the protein may have adapted to utilization of reduced flavin as an electron donor.

For determining the two-electron midpoint potential of the PqsL-internal FAD, we used an assay based on the method published by Massey (22). In brief, xanthine oxidase is used to reduce PqsL as well as a reference dye with known redox potential. From ratios between oxidized and reduced species, the redox potential of the PqsL-internal flavin can be derived. Of the three reference dyes tested, only indigo carmine (E_{m7} = −125 mV; where E_{m7} indicates the midpoint potential at pH 7) was suitable for the competitive reduction experiment, whereas phenosafranine (E_{m7} = −252 mV) and anthraquinone (E_{m7} = −184 mV) potentials were too negative. Exemplary spectra, including the respective least-squares fits, are shown in Fig. 2*A*. Spectra of oxidized and reduced species of PqsL and indigo carmine used for the fit are shown in Fig. S1. The kinetics of the reaction is displayed in Fig. 2*B*. Based on the linear fit within the Nernst plot shown in Fig. 2*C*, a midpoint potential of −140 ± 4 mV was calculated for PqsL (not taking in account slight deviations due to pH). Hence, PqsL features a rather positive midpoint potential compared with other class A monooxygenases. Although it is debatable whether this could be interpreted as an adaptation to an alternative electron donor, it can certainly be concluded that, electrochemically, efficient reduction of PqsL by reduced flavin is feasible.

FAD reductase HpaC supports PqsL activity in the coupled PqsL/PqsBC assay

Because of its sensitivity to oxidation, chemically prepared $FADH_2$ as electron donor for PqsL is highly inefficient and inconvenient for use in enzyme assays. We therefore searched for other ways to promote the PqsL-reductive half-reaction. It turned out that in an assay where PqsL, PqsBC, 2-ABA, octanoyl-CoA, and NADH were provided, addition of either cell-free extracts or cell-free extracts depleted of dissolved low molecular weight substances of either *P. aeruginosa* PAO1 or

Escherichia coli DH5α led to the formation of small amounts of HQNO (<5 μM). This suggested that a protein rather than an additional low-molecular weight compound supported PqsL activity, either by transferring electrons from NADH to PqsL or, more likely, by providing free reduced FAD. Such a reaction scheme has previously been reported for flavin-dependent halogenases that have structural similarity to group A flavoprotein monooxygenases (both share a GSH reductase fold) and require the supply of reduced flavin for enzyme activity (27). In several cases, these proteins are not associated with a cognate flavin reductase (19, 28), as observed for two-component monooxygenases like StyAB or HpaAC (28–30).

The genome of *P. aeruginosa* PAO1 contains several predicted flavin reductase genes, but FAD reductase activity has only been confirmed for HpaC (PA4092). HpaC is the 18-kDa reductase protein of the two-component monooxygenase system HpaAC, which catalyzes the hydroxylation of *p*-hydroxyphenylacetate (pHPA), and is conserved in both *E. coli* and *P. aeruginosa* (29). HpaC of *P. aeruginosa* reduces FAD with NADH and releases the $FADH^-$ product into solution (31). Remarkably, the activity of HpaC of *P. aeruginosa* is not influenced by the monooxygenase substrate pHPA, (31), as this is the case in the HpaAC homologs of *Pseudomonas putida*, *Acinetobacter baumannii,* or *E. coli* (32–34). This property makes HpaC an ideal supporting enzyme for *in vitro* characterization of the PqsL reaction.

HpaC was purified as a pale-yellow protein with ~1% of protein molecules carrying a flavin cofactor according to spectroscopic analysis. Its reductase activity, monitored by following NADH oxidation in a spectrophotometric assay, was consistent with previously reported data (31). We first investigated whether HpaC was capable of reducing the PqsL-bound FAD. To this end, anoxic solutions of PqsL and HpaC (10,000:1 molar ratio) were mixed, and the flavin bleaching upon addition of NADH was monitored at 448 nm. The instantaneous reduction of PqsL observed suggests that either HpaC is able to directly reduce the PqsL-bound FAD or residual free reduced FAD serves as a catalyst for a very efficient diffusion-based reduction.

In accordance with the observed reduction of PqsL, small quantities of HpaC supported HQNO formation in the coupled PqsL/PqsBC reaction (Fig. 3). Although the reaction showed a clear dependence on the amounts of each individual enzyme used, catalytic amounts of FAD had a positive effect on HQNO yields. In contrast, excess FAD, particularly in conjunction with excess HpaC, rendered the reaction inefficient. This can be explained by oxygen depletion due to hydrogen peroxide formation out of $FADH_2$ autoxidation, a notion that is supported by the observation that catalase, which produces one O_2 from two H_2O_2, rescued the reaction to some extent (Fig. 3*E*). Because HQNO yields decreased considerably when NADH concentrations were reduced in the assay, it can be assumed that the reaction is rather inefficient *in vitro*. This may be due to the short lifetime of reduced flavin in the presence of oxygen (35) and the possibility that PqsL, similar to other group A monooxygenases, is incapable of sustaining a reactive flavin intermediate in the absence of substrate. In contrast, *e.g.* the oxygenase subunits of two-component monooxygenases, in which the C(4a)-hydroperoxyflavin is preserved to some extent, group A monooxygenases regulate FAD reduction depending on the presence of substrate (21, 33). The data presented in Fig. 3 of course raise the question of how a PqsL-reductase system can function efficiently *in vivo*. Although we cannot offer any explanation so far, we hypothesize that reduced flavin may behave differently in the cellular environment. Moreover, the benefit of a flexible enzyme system, with a monooxygenase that can accept reduced FAD as well as FMN from different reductases, might outweigh the disadvantage of increased formation

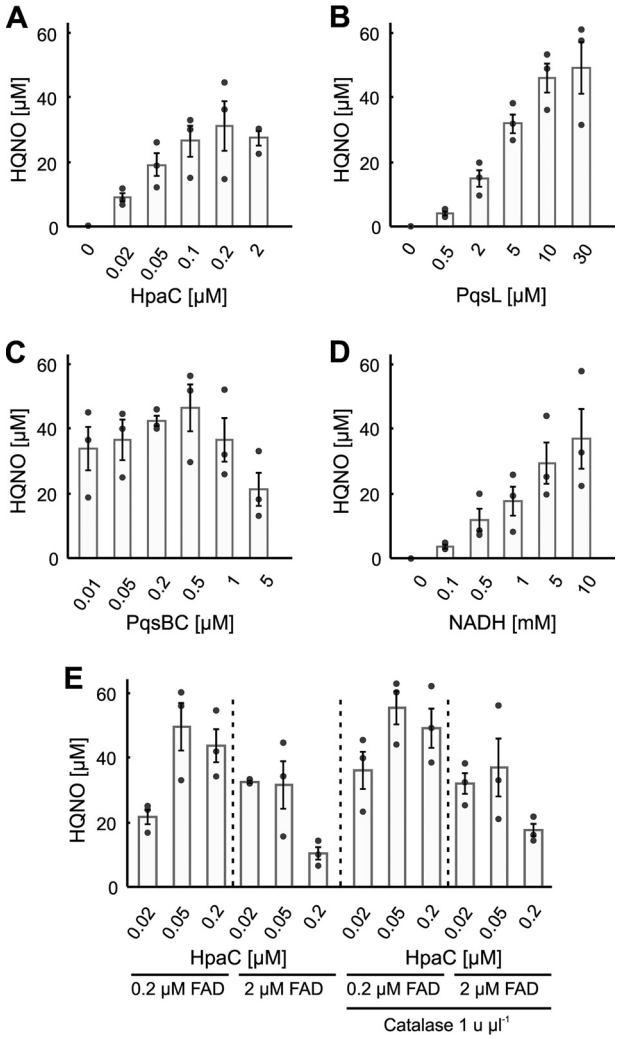

Figure 3. HQNO formation in the coupled PqsL/PqsBC reaction as a function of individual components of the assay. Reactions were run for 2 h for complete conversion of PqsBC substrates before products HHQ (not shown) and HQNO were extracted with ethyl acetate and analyzed by HPLC. *A*, 5 μM PqsL was incubated with varying concentrations of the FAD reductase HpaC, 0.5 μM PqsBC, 100 μM 2-ABA, 120 μM octanoyl-CoA, and 5 mM NADH. *B,* PqsL was varied; concentrations are as in *A* but with 0.2 μM HpaC. *C,* variation of PqsBC shows that excess PqsBC depletes 2-ABA before conversion by PqsL, leading to a decrease in HQNO (conditions are as in *A* but with 0.05 μM HpaC and 0.2 μM FAD). *D,* variation of NADH illustrates the inefficiency of the reaction *in vitro* (conditions are as in *A* but with 0.2 μM HpaC). *E,* supplementation with 0.2 μM FAD increases reaction efficiency and requires less HpaC for efficient HQNO formation (NADH was 5 mM). Excess of FAD (2 μM series) decreases the yield. To confirm that oxygen depletion by FADH2 autoxidation was the cause of reduced product formation, the experiment was repeated with catalase supplementation (*right side*). Oxygen recovery out of H_2O_2 by catalase leads to an increase of reaction efficiency. *Error bars* represent standard deviations.

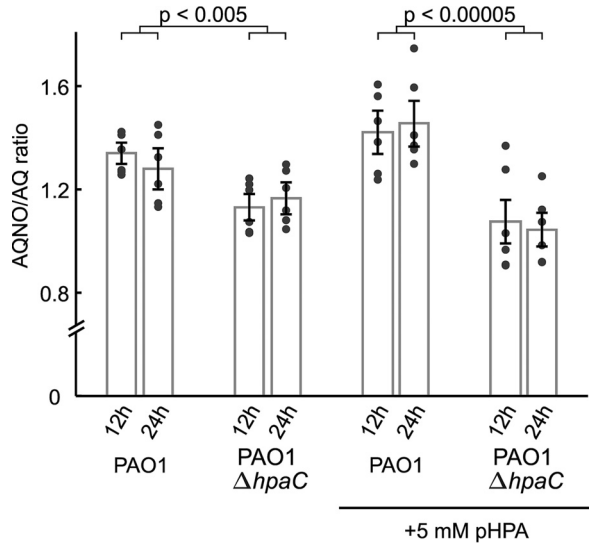

Figure 4. Impact of the deletion of *hpaC* on the production of AQ and AQNO. *P. aeruginosa* strains PAO1 and PAO1 Δ*hpaC* were cultivated in LB medium with 2 mM anthranilic acid at 37 °C. AQ and AQNO were quantified by HPLC for 12 and 24 h after inoculation, and ratios between AQs and AQNOs were calculated. Supplementation of media with 5 mM *p*-hydroxyphenylacetic acid (*pHPA*, indicated) led to different effects in both strains. *Error bars* represent standard deviations.

of reactive oxygen species from free reduced flavin. Low efficiencies in NADH utilization and high rates of autoxidation have also been reported for *in vitro* assays with designated two-component monooxygenases and halogenases (29, 32, 33, 36, 37).

Deletion of hpaC in P. aeruginosa PAO1 influences the HQNO to HHQ ratio

The *pqsL* gene is not clustered with any flavin reductase gene. This is not utterly uncommon for enzymes utilizing reduced flavin as electron donor, and in the respective cases, the cognate reductase is unknown (38). Because the *in vitro* activity of PqsL was supported by HpaC, we were interested in whether the *hpaC* gene of *P. aeruginosa* can be linked to AQNO levels *in vivo*. Analyzing available transcriptomic data, *e.g.* from the NCBI GEO database, no connection between *hpaC* and *pqsL* expression levels was found. However, because no clear induction of *pqsL* under any conditions has been observed, it is possible that its activity is not primarily regulated on a genetic level, but rather by substrate/co-substrate availability.

Reduced flavins are produced from an array of enzymes involved in various processes (42). *P. aeruginosa* features at least one additional flavin-reducing enzyme whose function has been proven experimentally, namely MsuE (PA3446). However, use of MsuE was precluded for the *in vitro* experiments of this study, because it possesses nitroreductase side activity (40), which might interfere with the hydroxylamine product of PqsL.

When growing *P. aeruginosa* PAO1 Δ*hpaC* in LB medium supplemented with 2 mM anthranilic acid, a decrease of AQNOs relative to AQs was observable compared with the PAO1 WT (Fig. 4). We then assayed the total FAD reductase activity of cell-free extracts of the WT strain and the Δ*hpaC* mutant, grown in the presence or absence of pHPA, the substrate of the HpaAC two-component monooxygenase. As shown in Fig. S2, supplementation with pHPA induced reductase activity severalfold in the WT strain, probably by up-regulation of *hpaAC* gene expression, but not in the deletion mutant. It was therefore not surprising that addition of 5 mM pHPA to the growth medium led to a slight increase in relative AQNO levels in the PAO1 culture (Fig. 4). In contrast, the Δ*hpaC* strain showed a further decrease, possibly due to the competition of PqsL and HpaA, the monooxygenase component of HpaAC, which presumably is also up-regulated in presence of pHPA, for the remaining free flavin. It has to be mentioned that the observed differences were not present when cultures were insufficiently aerated or when media were not supplemented with the AQ precursor anthranilic acid, which boosts AQ productions (41). Hence, although not being evidence for physiologically relevant dependence of PqsL on HpaC, the data clearly support the hypothesis that free reduced flavin is the electron donor to PqsL *in vivo*.

PqsL releases 2-HABA, another substrate of PqsBC

The coupled enzyme assay involving PqsL and PqsBC, described above, did not indicate how and in which order both enzymes act in forming HQNO. To identify a reaction product released by one of the enzymes and converted by the other, PqsL and PqsBC reactions were separated by a dialysis membrane. Pretests showed that, despite the 3-kDa MWCO specification, besides molecular oxygen, only 2-ABA was able to efficiently pass the membrane (90% equilibrium after 15 min), whereas NADH, acyl-CoA, HHQ, and protein diffusion was not detected (diffusion monitored by UV spectroscopy, data not shown).

Despite the separation of PqsBC and PqsL, an average yield of 62 ± 9% (S.E., three experiments) HQNO was observed, suggesting that a diffusible compound is exchanged between PqsL and PqsBC. Because this compound is stable enough to survive transfer through the membrane for being converted by the downstream enzyme, the hypothetical PqsBC condensation product 1-(2-aminophenyl)decane-1,3-dione, whose half-life was below detection limit (UV spectroscopy, steady-state kinetics (42), and unpublished MS[4] and spectroscopic data), can most likely be excluded. This leaves the hydroxylated form of 2-ABA as the only plausible intermediate.

An additional outcome of the dialysis experiment was that, despite compartmentalization, relatively high yields of HQNO were achieved (the one-compartment reactions reached close to 60% only when enzyme and cofactor balance were optimal, Fig. 3*E*). The contrary would have been expected given the fact that osmotic permeation is a slow process, and besides the hypothetical 2-HABA, 2-ABA would also diffuse out of the PqsL compartment. A conceivable but admittedly speculative explanation would be that PqsL is inhibited by its own product. With the hydroxylation product diffusing out of the compartment, feedback inhibition would be lower than in a single compartment setup and therefore lead to higher production of HQNO (which is also promoted by 2-HABA being preferentially converted by PqsBC, see below). However, given the complexity of the reaction and the instability of cofactors and sub-

[4] S. L. Drees and S. Fetzner, unpublished data.

strates involved, performing kinetic analyses of the system to assess product inhibition of PqsL is not feasible.

To verify 2-HABA formation, we attempted to track down the direct product of the PqsL reaction by HPLC. By injecting a sample containing PqsL, HpaC, NADH, and 2-ABA to HPLC immediately after starting the reaction, an additional compound could indeed be observed (Fig. 5*A*). From the retention time and UV absorption characteristics (Fig. 5*B*), it seemed likely that the compound was a derivative of 2-ABA. When this compound was isolated from the HPLC eluate and directly converted by PqsBC with octanoyl-CoA, HQNO was detected as sole reaction product, indicating that the compound must be 2-HABA. For further verification, 2-HABA was produced by chemical synthesis. To this end, 2-nitrobenzoylacetate (2-NBA) was partially reduced using zinc dust under argon atmosphere. This approach was described previously for production of hydroxyarylamines (43, 44). Reactions were conducted in an aqueous buffer because the amino-derivative, 2-ABA, rapidly decomposes in all solvents except for water (42). Typical yields of 2-HABA were around 30% according to HPLC analysis (estimated from peak area at 360 nm), with minor amounts of 2-ABA formed. As shown in Fig. 5*A*, the chemically synthesized 2-HABA had the same retention time as the compound released by PqsL; moreover, UV spectra were identical (data not shown). However, we were not able to unambiguously identify a mass corresponding to 2-HABA by HPLC-MS. Using repeated HPLC injections, it was possible to estimate its stability (Fig. 5*C*). Assuming a first-order reaction, a half-life of 16.2 min was estimated for both synthetic and enzyme-produced 2-HABA. We observed minor amounts of 2-NBA and 2-ABA (~10% peak area) as potential decomposition products, as well as a number of additional unidentified compounds. Because hydroxyarylamines are highly nucleophilic and can undergo a variety of reactions (45), we suggest that 2-HABA forms various products, depending on which reaction partners are available.

For further verification of 2-HABA authenticity, we employed a derivatization intended to stabilize the hydroxylamine group. It was demonstrated before that amines and hydroxylamines can react with acetic anhydride at 0 °C and strongly acidic pH to *N*- and *O*-acetylated products, respectively (46). We adopted the procedure for derivatization of 2-ABA and 2-HABA, using an alkaline buffer, which acidified during the reaction due to anhydride decomposition. This modification was required to maintain stability of the starting materials. The reaction and potential reaction products are shown in Fig. 5*D*. Although the efficiency of the reaction was greatly reduced under the conditions used, we were able to identify compounds with molecular masses corresponding to those of the postulated acetylated products. Extracted ion chromatograms of the positive ion mode MS are shown in Fig. 5*E*. The data verified the presence of the hydroxylamino group in 2-HABA; however, due to the low efficiency of the derivatization, the procedure is not suitable for quantitative measurements, such as enzyme kinetics.

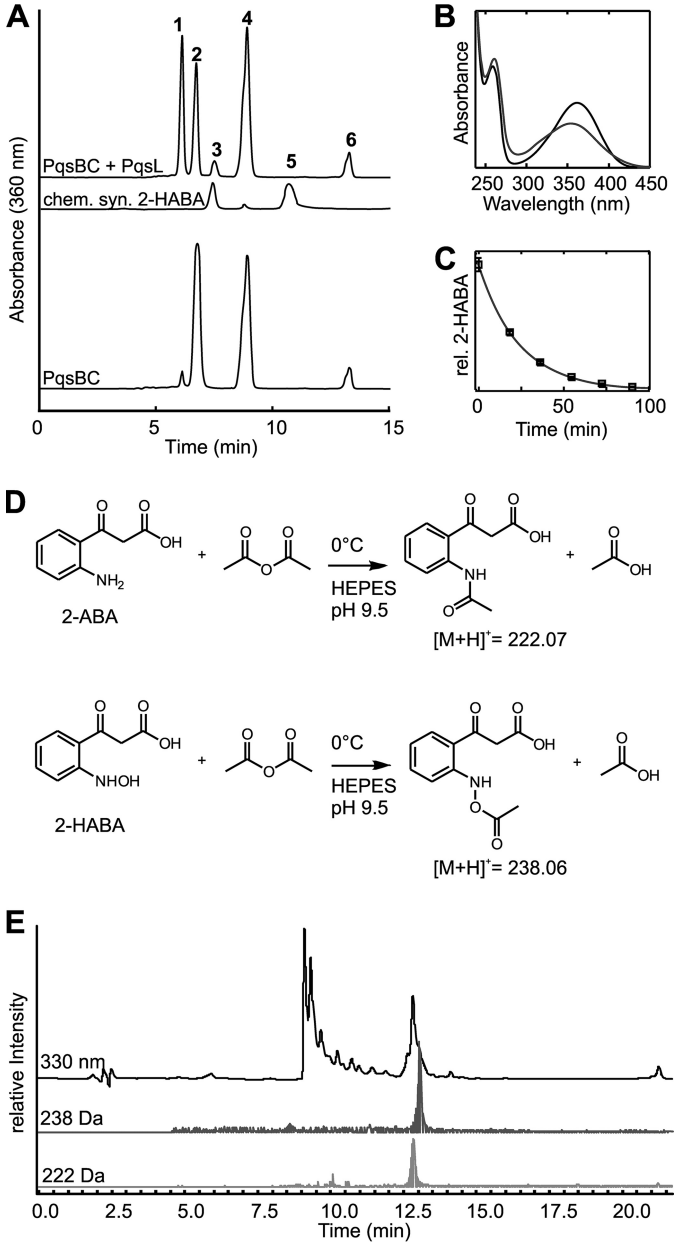

Figure 5. Identification of the PqsL reaction product 2-HABA. *A,* diagram shows chromatograms (stacked) of enzyme assays (*top*) and chemically synthesized (*chem. syn.*) 2-HABA (*middle*) from reverse-phase HPLC. Control experiments (*e.g.* using PqsBC, *bottom trace*) and spectra comparisons (not shown) allow the assignment of peaks to the following: *1,* NAD; *2,* NADH; *3,* 2-HABA; *4,* 2-ABA; *5,* 2-NBA; *6,* 2-AA. For confirmation of 2-HABA authenticity, peak 3 was prepared and converted with PqsBC to yield exclusively HQNO (not shown). *B*, comparison of normalized UV absorption spectra of 2-HABA (*gray*) and 2-ABA (*black*) as recorded with the HPLC diode array detector. *C,* decomposition of 2-HABA determined with HPLC. *Error bars* reflect standard error of mean (three representative replicates of synthetic and enzymatically prepared 2-HABA). Data were fitted with one exponential function (*gray line*) revealing a half-life of 16.2 ± 0.1 min. *D,* reaction schemes of derivatizations of 2-ABA and 2-HABA with acetic anhydride. *E,* LC-MS identification of the products of derivatization (according to *D*) of 2-ABA and of the of PqsL reaction products. *Upper trace* shows UV absorbance as measured with the LC-MS DAD detector; *middle* and *lower traces* show extracted ion chromatograms of the denoted masses of the positive MS.

2-HABA is preferred over 2-ABA by PqsBC

The observation that PqsBC catalyzes the condensation of octanoyl-CoA with either 2-ABA or 2-HABA raises the question of which substrate is preferred by the enzyme. The preference of PqsBC is a critical factor for the balance between AQ and AQNO, which are produced in comparable quantities by *P. aeruginosa* (1, 14). Because it was impossible to isolate and handle 2-HABA without significant decomposition, determin-

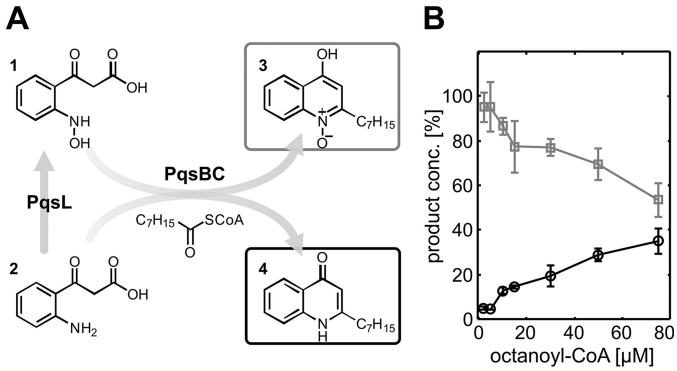

Figure 6. Substrate preference of PqsBC. *A,* reaction scheme on the *left* illustrates the two substrates 2-ABA (*1*) and 2-HABA (*2*), with the latter being generated *in situ* by PqsL at a constant rate (additionally required substrates NADH, O_2, and the supporting enzyme HpaC were left out for clarity). Depending on its substrate preference, PqsBC converts either compound to the respective product (*3,* HQNO; *4*, HHQ) until octanoyl-CoA is depleted. *B,* dependence on octanoyl-CoA hence reveals which substrate, 2-ABA or 2-HABA, is the preferred and/or more efficient one. Initial 2-ABA concentration was 250 μM. HQNO, *gray*; HHQ, *black*. *Error bars* reflect S.E. of three independent replicates.

ing the specificity constant $k_{cat}\ K_m^{-1}$ of PqsBC for the two substrates by steady-state kinetics was not feasible. An alternative approach was therefore employed using the combined PqsL–PqsBC assay in which 2-ABA and 2-HABA (produced by PqsL *in situ*) were offered in excess, whereas octanoyl-CoA, the second substrate of PqsBC, was limited. Whichever substrate is preferred by PqsBC will be converted until all octanoyl-CoA is used up (reaction scheme displayed in Fig. 6*A*). Varying the octanoyl-CoA concentration can therefore provide an estimate of which compound is the preferred substrate to PqsBC. Comparable assays were used for analyzing the conversion of competing substrates, and simulations were undertaken to understand the kinetics underlying the enzymatic conversion of competing substrates (47–50).

We set up a system in which approximately equal initial concentrations of both substrates were generated in the assay. This was indicated by the observation that equal amounts of HHQ and HQNO are formed when a huge excess of octanoyl-CoA and PqsBC is added to the reaction. The pattern displayed in Fig. 6*B* clearly suggests that conversion of 2-HABA is far more effective than conversion of 2-ABA. However, the experimental setup does not allow us to conclude whether this is due to a higher affinity or a more efficient turnover.

With respect to the physiological context, the higher efficiency of 2-HABA conversion would also make sense because 2-HABA as a primary aromatic hydroxylamine (*N*-aryl hydroxylamine) is highly reactive toward DNA, nucleotides, and presumably other biomolecules (51). *N*-Aryl hydroxylamines or their metabolic successors have been demonstrated to possess genotoxicity in several studies (52–55). The efficient downstream conversion of 2-HABA may therefore be important for protecting *P. aeruginosa* from cellular damage.

Analysis of the PqsL crystal structure supports a dysfunctional NAD(P)H-binding site

To resolve why PqsL, despite being closely related to NAD(P)H-dependent pHBH-type monooxygenases, would accept neither co-substrate, we performed an in-depth analysis of the crystal structure of PqsL and compared its putative co-substrate-binding region to that of pHBH of *Pseudomonas fluorescens* (PDB code 1PBE), the model enzyme of the group A monooxygenase subfamily (27). In the first step, we used the PqsL structure (PDB code 2X3N), which was solved to a resolution of 1.75 Å by Naismith and co-workers (16), and remodeled a loop region, which aligns with a loop reported to be involved in NADPH and FAD binding in pHBH (Fig. 7*A*). As confirmed by the $2F_o - F_c$ map calculated by using the published structure factors of 2X3N, the 40–44 loop region of the PqsL was not interpreted in the first place due to poor electron density (Fig. S3*A*). By using the electron density from the OMIT map density-modification strategy (Fig. S3*B*), we were able to complete the loop (Fig. S3*C*), obtaining structural information on the cofactor-binding mode, although some residues, such as Ala-42, showed incomplete electron densities.

Interestingly, the PqsL-bound FAD shows a slight deviation from the planar geometry of the isoalloxazine in the 2X3N model, which can be justified by the electron density observed. Such a distortion could result from X-ray radiation damage, so that the protein-bound flavin is reduced *in situ* to some extent. However, density modification improved the resolution around the flavin, so a planar geometry of the isoalloxazine is conceivable as both the crystallographic reality and the native cofactor conformation. The refinement has been deposited in the Protein Data Bank as 6FHO.

pHBH is thoroughly studied with respect to its reaction mechanism, as well as substrate and co-substrate binding. Despite limited sequence similarity, its structure is very similar to PqsL (root mean square deviation of 2.4 Å with 394 of 399 residues aligned, 19% sequence identity). Both proteins share a GSH reductase fold with one Rossmann fold for binding FAD. In contrast to other NAD(P)H-utilizing proteins, pHBH-like enzymes do not feature a designated NAD(P)H-binding domain, but instead they use a loop substructure and several residues on both sides of the FAD-binding ridge for interaction with the co-substrate (18, 56–59). Both enzymes, PqsL and pHBH, comprise the fingerprint motif (^{2}*GXGXXG*^{17} in PqsL) for binding the FAD adenine moiety and the highly conserved DG motif (^{159}DG^{160}) that was demonstrated to interact with both NADPH and FAD in pHBH (59). PqsL also shares a glutamic acid (Glu-35), conserved in several pHBH homologs within the Rossmann fold, that interacts with the FAD ribose. In contrast, a conserved arginine in proximity of the adenine, involved in NADPH binding in pHBH (Arg-33) (57), is altered for a glutamine (Gln-36). Additionally, NADPH transiently interacts with the loop of pHBH that aligns with the remodeled PqsL loop (58). This substructure is shorter in PqsL, and a helix present within this loop in pHBH (helix H2, residues 33–40 in pHBH) is broken up. To compare the key residues for NAD(P)H binding in pHBH with those in the PqsL structure, the two structures are superposed in Fig. 7*C*. A table with the key residues structurally aligned between the two proteins is shown in Fig. 7*A*.

Two residues in the loop were demonstrated to be essential for the reductive half-reaction in pHBH as well as for NADPH specificity, Arg-42 and Tyr-38 (57, 60). Although Arg-42 interacts with the ribosyl alcohols of the FAD adenosine nucleotide

A

	1	2	3	4	5
PqsL	R_{41}	I_{43}	A_{164}	G_{275}	G_{45}
PHBH	Y_{38}	R_{42}	H_{162}	R_{269}	R_{44}

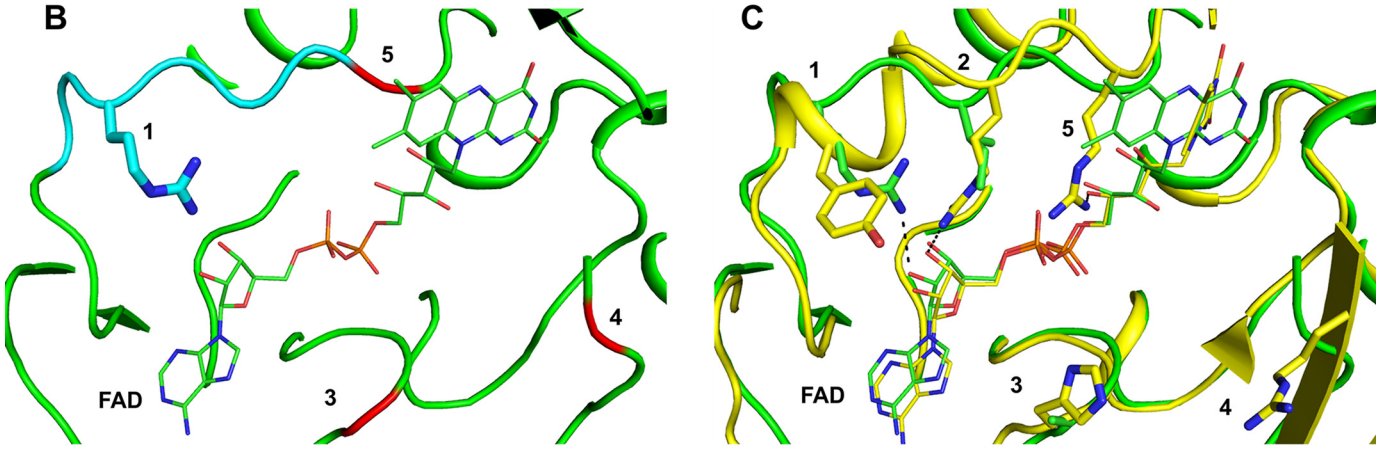

Figure 7. Structural investigation of co-factor and co-substrate binding in PqsL. *A,* survey of key residues for NADPH interaction in pHBH and corresponding residues of PqsL, as deduced from the structural alignment of PqsL with pHBH. *B,* view of the 6FHO model (*green*) with the remodeled loop (*cyan*). Positions involved in NADPH recognition in pHBH that likely are dysfunctional in PqsL are highlighted in *red*: Arg-41 (*1*), which aligns with Tyr-38 of pHBH and adopted the function of Arg-42 (*2*) of pHBH (see *C*) is shown in *stick* representation. *C,* close-up of the flavin-binding site of PqsL (*green*) aligned with pHBH (1PBE, *yellow*).

and supposedly is mandatory for positioning the FAD, Tyr-38 may directly or indirectly interact with NADPH (58, 61). It is therefore not surprising that the ribosyl-coordinating Arg-42 is functionally conserved in PqsL (Arg-41), whereas Tyr-38 is not. Notably, Arg-41 of PqsL has a different conformation than Arg-42 of pHBH and does not align with Arg-42 but with Tyr-38 of pHBH (Fig. 7*C*, *#1* and *#2*). It is therefore questionable whether Arg-41 of PqsL, despite its different position within the loop, is capable of supporting NAD(P)H binding via 2′-phosphate recognition in a similar way as has been reported for pHBH (57). Fig. 7*C* illustrates the conformational differences in both structures that could be resolved by reevaluation of the 2X3N crystal structure. The remodeling of the loop with the respective electron density maps is shown in Fig. S3.

Located on the opposite side of the FAD-binding cleft, Arg-269 and His-162 of pHBH were proven to be essential for NADPH oxidation while not affecting hydroxylation. These two residues align with Ala-164 and Gly-275 in PqsL (Fig. 7*C*, *#3 and #4*), which are unable to support the same interactions (Fig. 7*C*, *#3 and #4*).

Crystallographic studies of the pHBH–NADPH complex moreover had illustrated the role of Arg-44 for both cofactor and NADPH binding (58). Without substrates bound (closed conformation), it forms hydrogen bonds with the diphosphate and with ribityl hydroxyls of the flavin nucleotide. In the co-substrate–bound form its conformation changes, allowing interaction with what appears to be the phosphoribose of NADPH. Strikingly, Arg-44 of pHBH seems to be substituted with a glycine in PqsL (Gly-45, Fig. 7*C*, *#5*). Gly-45 interacts by means of a peptide bond–aromatic interaction with the isoalloxazine moiety of FAD (distance between NH and the center of the carbocyclic aromatic ring is in agreement with calculations by Bendová *et al.* (62)). Although this interaction is rather weak, it is potentially crucial for orienting the flavin at its position because in pHBH the FAD open conformation is retained by van der Waals interaction of the flavin with Arg-44 (63). The PqsL flavin is furthermore stabilized by hydrophobic interactions with Ile-272 and Pro-273, as well as by hydrogen bonds of the Pro-299 and Gly-304 backbone amide groups to N3 and the C2 carbonyl, respectively. Notably, the flavin conformation found in PqsL cannot be classified in analogy to the open and closed orientations found in pHBH. Structural alignments suggest that the conformation found in PqsL is closer to the "open" state, which is rather unusual for a group A monooxygenase without substrate bound (see Fig. S4). However, there is no apparent space for a conformational change within the structure for the flavin to move into a "closed" conformation, as this is the case in pHBH (63, 64). Moreover, due to the above-mentioned differences, the FAD-binding pocket is widened, and the flavin is more exposed than in related enzymes. Lacking coordination, the FAD possesses a higher degree of conformational freedom, possibly for enhancing electron uptake from reduced flavin.

Taken together, the available structural data on PqsL support the hypothesis that the enzyme is not capable of binding NAD(P)H in the alleged mode because several of the crucial positions are replaced by dysfunctional substitutions. However, provided that PqsL indeed binds reduced FAD in lieu of NAD(P)H, instead of exchanging its cofactor, it remains to be elucidated how PqsL facilitates electron transfer and whether different flavin conformations are involved in controlling the catalytic reaction.

Unfortunately, pHBH is the only group A monooxygenase that has been extensively studied with respect to co-substrate recognition. The sequence diversity among even closely related enzymes of the subclass and the rather few determinants for co-substrate binding calls for additional studies employing other enzymes to recognize recurring binding patterns. There

might even be flavin monooxygenases with promiscuous co-substrate utilization, utilizing both reduced flavin and NAD(P)H. It is known that flavin-dependent monooxygenases can be very efficient catalysts, *e.g.* >50 turnovers are reached by pHBH (21, 56). Although this is desirable in degradation processes, in the case of PqsL the balance between AQ and AQNO pathway products would be disturbed by excess PqsL activity. Whereas intracellular pools of NADH and NADPH are readily accessible and millimolar cellular concentrations were determined for *E. coli* (65), reduced flavin, due to its potential to generate reactive oxygen species, is not relied on as a default reducing agent in the cell and is probably much less available. Little is known about the regulation and total concentrations of intracellularly reduced flavin (39); still, it is conceivable that its use as an alternative electron donor is more widespread than expected so far.

Experimental procedures

Preparation of cell extracts and protein purification

Cell extracts were produced from *E. coli* DH5α, *P. aeruginosa* PAO1, or *P. aeruginosa* PAO1 Δ*hpaC* by sonicating 1 g of cells ml^{-1} four times for 2 min in 50 mM Tris-Cl, pH 7.5. Lysates were cleared by centrifugation (25,000 × *g*, 4 °C, 40 min), filtered through 0.22-μm filters (VWR, Radnor, PA), and flash-frozen in liquid nitrogen until further use. Alternatively, for removal of low-molecular weight compounds, cell extracts were run through 5-ml size-exclusion columns (HiTrap desalt, containing Sephadex G-25 Superfine, GE Healthcare) equilibrated with 50 mM Tris-Cl, pH 7.5, prior to freezing in liquid nitrogen.

Proteins were heterologously overproduced in *E. coli* Rosetta2 pLysS (Merck Millipore, Billerica, MA) and transformed with pET28b or pET23a expression vectors containing the respective genes. For production of PqsL and HpaC, the respective recombinant strains were grown at 37 °C in LB medium to an A_{600} of 0.5, then cooled down to 20 °C for 20 min before inducing overexpression with 0.5 mM isopropyl 1-thio-β-D-galactopyranoside. After overnight incubation, cells were harvested by centrifugation (15 min, 6000 × *g*) and frozen at −80 °C until further use. For preparation of cell-free protein extracts, pellets were thawed, suspended in 20 mM Tris-Cl, pH 8, 150 mM NaCl, and 0.1% Nonidet P-40, and sonicated for four times for 2 min. Lysates were centrifuged (40 min, 25,000 × *g*, 4 °C) and filtered through a 0.45-μm polyvinylidene difluoride syringe filter (Carl Roth, Karlsruhe, Germany). PqsL was purified by means of either a hexahistidine or a StrepII tag fused to the N terminus. Immobilized metal-affinity chromatography was carried out with 1 ml of HisTrap FF columns and Äkta Prime plus automated chromatography units for gradient elution (both from GE Healthcare). Purification of StrepII-tagged PqsL was performed using a 1-ml Strep-Tactin-Sepharose column (IBA Life Sciences, Göttingen, Germany) with a washing buffer containing 20 mM Tris-Cl, pH 8, and 150 mM NaCl. Elution was conducted using 2.5 mM *d*-desthiobiotin in the same buffer. Subsequent to affinity chromatography, the prepared proteins were buffer-exchanged into 20 mM HEPES, pH 8, and 50 mM NaCl using HiTrap desalt columns (GE Healthcare) and concentrated to more than 10 mg ml^{-1} with 10-kDa MWCO centrifugal concentrators (Sartorius, Göttingen, Germany). HpaC was purified with a C-terminal hexahistidine tag according to Ref. 31; PqsD, PqsE, and PqsBC were purified as reported previously (42, 66). For all proteins, 10% glycerol was added as cryoprotectant before flash-freezing protein aliquots in liquid nitrogen for later use.

Cultivation of *P. aeruginosa* PAO1 and PAO1 Δ*hpaC* for FAD reductase assays

P. aeruginosa PAO1 WT and the *hpaC* deletion strain were pre-grown in LB medium before a 1:1000 dilution into M9 minimal medium with 10 mM succinate as the sole carbon source. 50 ml of overnight cultures were harvested and subsequently resuspended in 50 ml of fresh M9 medium supplemented with either 10 mM succinate or 0.5 mM succinate and 10 mM pHPA. Cells were then grown for another 3 h, harvested by centrifugation (6000 × *g*, 10 min), and stored at −80 °C until further use.

Synthesis of anthraniloyl-CoA, 2-ABA, and 2-HABA

Anthraniloyl-CoA and 2-ABA were prepared as described previously (42, 66). For preparation of 2-HABA, 5 mg of 2-NBA, prepared according to Refs. 42, 67–69, were dissolved in 1 ml of ice-cold 20 mM Tris base solution, pH 9.5 (Carl Roth). 10 mg of zinc powder and a magnetic stirrer were added, and the suspension was vigorously stirred for 30 min at 0 °C under an argon atmosphere (1 bar overpressure) for reduction of the nitro group (43, 44). Longer incubation times did not lead to increased yields of 2-HABA. The suspension was passed through a glass frit and a 0.45-μm filter and immediately subjected to preparative HPLC.

Derivatization of 2-HABA and 2-ABA

2-ABA and unstable 2-HABA produced by PqsL were derivatized according to a procedure used by Lee and co-workers (46), in which aromatic amines and hydroxylamines are reacted with acetic anhydride. The reaction was performed in 50 mM HEPES, pH 9.5, on ice to slow down decomposition of the compounds. After addition of acetic anhydride to a final concentration of 1% (v/v), the mixtures were kept on ice for another 30 min and centrifuged to remove precipitated protein. After filtration through a 0.45-μm filter, samples were analyzed with LC-MS.

HPLC and HPLC-MS analysis of reaction products

All HPLC experiments were performed with an Agilent 1100 Series instrument (Agilent, Santa Clara, CA) equipped with autosampler, binary pump, and diode array detector. Knauer Eurospher II 4 × 150-mm C18 and C18-H columns (Berlin, Germany) were used for all experiments. For preparation of chemically synthesized 2-HABA or for analysis of PqsL reaction products, separation of 2-ABA, 2-HABA, 2-NBA, and 2,4-dihydroxyquinoline was performed using a 20 mM ammonium carbonate buffer, pH 8.7, as solvent A and acetonitrile (both Carl Roth) as solvent B. Elutions were started with 1 min of isocratic flow (100% A) before linearly increasing to 20% B over 12 min. B was then increased to 80% over 5 min. The flow rate was kept constant at 0.8 ml min^{-1}.

HPLC analyses of AQ reaction products were conducted as described previously (66). In brief, solvents were 6 mM aqueous citric acid (A) and methanol (B) with a gradient from between 10 and 40% B to 100% B. HHQ and HQNO were quantified from calibration with the commercially available authentic compounds, detected at 315 and 326 nm, respectively (Sigma and Santa Cruz Biotechnology, Dallas, TX).

HPLC-MS analysis of 2-ABA, 2-HABA, and their derivatives was performed using a procedure described before for HHQ using a Thermo Fisher Scientific Ultimate 3000/Bruker Amazon speed instrument (66). To increase the sensitivity for detecting labile compounds, electrospray ionization parameters were varied according to the manufacturer's recommendations.

UV spectroscopic enzyme assays

For the detection of substrate, NAD(P)H:oxygen oxidoreductase activity of PqsL, the oxidation of either NADH or NADPH was monitored spectrophotometrically at 340 nm as a function of the potential substrates anthranilic acid (Sigma), anthraniloyl-CoA, and 2-ABA. Assays were conducted in 20 mM HEPES or Tris-Cl, pH 8.0, and contained 0.1 to 20 μM PqsL, 100 μM substrate, and 100 μM of either NADH or NADPH (Sigma). Additives were PqsD, PqsE, or PqsBC (up to 10 μM), 100 μM malonyl-CoA, and 100 μM octanoyl-CoA (both from Sigma). Absorbance changes were measured for up to 30 min (V-550 or V-750 spectrophotometers, Jasco, Tokyo, Japan, or Evolution 201 UV-visible spectrophotometer, Thermo Fisher Scientific). For anoxic measurements, assays were prepared in an anaerobic chamber in a gas-tight microcuvette (Hellma Analytics, Mülheim, Germany). PqsL was chemically reduced by titration with a solution containing 50 mM Tris-Cl, pH 8, and 1 mM sodium dithionite (Sigma). Single turnover experiments were conducted by injecting air-saturated solutions containing the substrate combinations denoted above. Flavin reductase assays with HpaC were conducted in 20 mM HEPES or Tris-Cl, pH 8.0, with 50 μM FAD or FMN (Sigma) as electron acceptor and between 5 and 100 μM NADH. Enzyme concentrations were varied between 0.1 nM and 1 μM.

Determination of the redox potential of PqsL-bound FAD

The redox potential of enzyme-bound FAD was determined employing xanthine oxidase as described previously (22). Xanthine oxidase oxidizes xanthine to uric acid and in the absence of oxygen provides electrons to redox dyes with a midpoint potential more positive than −410 mV. In the presence of two or more redox dyes, the more positive acceptor is favored. Combining PqsL and a dye with known potential, the redox potential of PqsL can be calculated according to the Nernst relation. Initial experiments indicated that PqsL had very limited stability in the assay. We therefore accelerated the reaction by increasing the concentration of xanthine oxidase in the assay, and we employed multivariate data analysis using component spectra to quantify reduced and oxidized states of PqsL and the respective dye. Assays contained 20 μM PqsL, different redox dyes (phenosafranine, $E_{m7} = -252$ mV; anthraquinone-2,6-disulfonate, $E_{m7} = -184$ mV; and indigo carmine, $E_{m7} = -125$ mV) in varying concentrations to give an absorbance between 0.1 and 0.5, 5 mM glucose, 10 μg ml^{-1} glucose oxidase, 5 μg ml^{-1} catalase, 200 μM xanthine, 2 μM benzyl viologen, and 200 nM xanthine oxidase (all Sigma) in 25 mM Tris-Cl, pH 8.0. Samples were set up in a sealable cuvette in an anaerobic chamber and incubated for 10 min at room temperature before starting the reaction by adding 3 μl of pre-diluted xanthine oxidase. Spectra were recorded every 15 s over 10 min at a scan rate of 6000 nm min^{-1}. Because of overlapping absorption peaks, concentrations of oxidized and reduced dye and PqsL were determined by least-squares fitting. Pre-recorded spectra of PqsL and the respective dyes in fully oxidized and reduced states served as composites for the fit. Calculations were performed with Matlab R2016B (The Mathworks, Natick, MA).

Multienzyme assays

Enzyme assays combining the PqsL and PqsBC reactions were performed using the stable AQ reaction products HHQ and HQNO as readouts, quantified by HPLC. PqsBC and PqsL concentrations were varied between 1 nM and 10 μM, and concentrations of substrates 2-ABA and octanoyl-CoA (Sigma), putative substrates NADH, NADPH, additives FAD, FMN, and additives catalase, PqsE, PqsD, and HpaC were varied. All assays were conducted in either 30 mM MOPS, pH 7.3, or 30 mM HEPES, pH 8.2, at 30 °C and 1000 rpm.

FAD reductase activity of cell extracts

Cell-free extracts were analyzed on FAD reductase activity with a spectrophotometric assay measuring the NADH-dependent reduction of FAD. To this end, protein concentrations were determined using a modified Bradford assay (70) and extracts were diluted to the same concentration with a buffer containing 30 mM Tris, pH 8, and 150 NaCl and stored on ice until used.

To minimize reoxidation of the reduced FAD, reactions were carried out in air-tight cuvettes and nitrogen-purged buffers and solution. Cell extracts were diluted into a buffer containing 30 mM Tris, pH 8, 150 mM NaCl, 1% (w/v) glucose, 25 units ml^{-1} glucose oxidase, and 250 units ml^{-1} catalase. 100 μM FAD was added, and the mixture was incubated at room temperature for 5 min. Reactions were started by addition of 1 mM NADH. FAD reduction was measured over 2 min at room temperature with a Jasco J-750 spectrophotometer. Initial rates were converted to specific activities using the extinction coefficient of $FAD_{ox\text{-}red}$ ($\epsilon_{450\ nm} = 10{,}600\ M^{-1}\ cm^{-1}$) (71).

Construction of the hpaC deletion mutant of P. aeruginosa PAO1

DNA manipulations were performed according to standard protocols. Genomic DNA of *P. aeruginosa* PAO1 was purified with the Puregene Tissue Core kit B (Qiagen, Hilden, Germany). Two PCR products spanning parts of the up- and downstream regions of *hpaC* were obtained from the genomic DNA of strain PAO1 with the primer pairs hpaC Up fw (5′-AAATCTAGACAACCTGTTCTGGTCGCTGA-3′)/hpaC Up rev (5′-GGGGATAACCTCCGAGGC-3′) and hpaC Dn fw (5′-CGCCTCGGAGGTTATCCCCACGGCGCCTCCAGGAATCC-3′)/hpaC Dn rev (5′-ATTAAGCTTCTATCGCCACGGCTTCTCCA-3′) and used as templates for a second overlapping PCR (SOE-PCR) (72) with the primers hpaC Up fw and hpaC Dn rev.

The resulting fragment was digested with XbaI/HindIII and ligated with the corresponding sites of the suicide vector pEX18Ap. The resulting plasmid was mobilized into strain PAO1 by triparental mating with *E. coli* strain DH5α as donor and strain HB101 pRK2013 as helper as described previously (73). Mutants were selected on *Pseudomonas* isolation agar plates containing 350 μg ml^{-1} carbenicillin and transferred onto LB plates containing 7% sucrose for selecting for vector excision by a second crossover. Single colonies were repeatedly streaked out and checked for gene deletion by PCR using the same primer pair as for the SOE-PCR. Finally, genomic DNA was purified from single mutant colonies and checked for gene deletion by PCR.

Refinement and analysis of the PqsL structure

The structure of the PqsL protein deposited in the Protein Data Bank (PDB code 2X3N) was used to analyze the interaction with its FAD cofactor. Because the structure lacks the residues between Glu-40 and Asn-44 that presumably play an important role in co-substrate recognition, the 2X3N protein model and structure factors were reprocessed. First, the $2F_o - F_c$ electron density map was inspected, and residues showing critical mismatches were removed from the model using Coot software (74). The structure was then refined using Refmac5 of the CCP4 crystallographic suite, and the residues thereby added again according to the $F_o - F_c$ Fourier map, slightly improving R and R_{free} values (75, 76). The omit map of the 40–44 loop, obtained by the Autobuild tool of Phenix crystallographic suite, was used as a map to fit the residues of the loop by means of the Phenix Fit Loop tool (77, 78). Finally, Refmac5 was run again to perform the final refinement of the whole model. PyMOL (Schrödinger, LLC) was used for alignments as well as analysis and visualization of the interactions between the protein and the FAD cofactor.

Author contributions—S. L. D. and S. F. conceptualization; S. L. D. validation; S. L. D., S. E., N. J., and U. H. investigation; S. L. D. visualization; S. L. D., S. E., B. D. B., N. J., and U. H. methodology; S. L. D. and S. F. writing-original draft; S. L. D., S. E., B. D. B., U. H., and S. F. writing-review and editing; B. D. B. formal analysis; S. F. supervision; S. F. funding acquisition; S. F. project administration.

Acknowledgment—We thank Prof. B. Philipp (University of Münster) for access to the electrospray ionization ion trap mass spectrometer (Deutsche Forschungsgemeinschaft Grant INST 211/646-1).

References

1. Lépine, F., Milot, S., Déziel, E., He, J., and Rahme, L. G. (2004) Electrospray/mass spectrometric identification and analysis of 4-hydroxy-2-alkylquinolines (HAQs) produced by *Pseudomonas aeruginosa*. *J. Am. Soc. Mass Spectrom.* **15,** 862–869 CrossRef Medline
2. Cao, H., Krishnan, G., Goumnerov, B., Tsongalis, J., Tompkins, R., and Rahme, L. G. (2001) A quorum sensing-associated virulence gene of *Pseudomonas aeruginosa* encodes a LysR-like transcription regulator with a unique self-regulatory mechanism. *Proc. Natl. Acad. Sci. U.S.A.* **98,** 14613–14618 CrossRef Medline
3. Pesci, E. C., Milbank, J. B., Pearson, J. P., McKnight, S., Kende, A. S., Greenberg, E. P., and Iglewski, B. H. (1999) Quinolone signaling in the cell-to-cell communication system of *Pseudomonas aeruginosa*. *Proc. Natl. Acad. Sci. U.S.A.* **96,** 11229–112234 CrossRef
4. Rampioni, G., Falcone, M., Heeb, S., Frangipani, E., Fletcher, M. P., Dubern, J.-F., Visca, P., Leoni, L., Cámara, M., and Williams, P. (2016) Unravelling the genome-wide contributions of specific 2-alkyl-4-quinolones and PqsE to quorum sensing in *Pseudomonas aeruginosa*. *PLoS Pathog.* **12,** e1006029 CrossRef Medline
5. Cooley, J. W., Ohnishi, T., and Daldal, F. (2005) Binding dynamics at the quinone reduction (Qi) site influence the equilibrium interactions of the iron sulfur protein and hydroquinone oxidation (Qo) site of the cytochrome bc_1 complex. *Biochemistry* **44,** 10520–10532 CrossRef Medline
6. Kita, K., Konishi, K., and Anraku, Y. (1984) Terminal oxidases of *Escherichia coli* aerobic respiratory chain. I. Purification and properties of cytochrome b_{562}-*o* complex from cells in the early exponential phase of aerobic growth. *J. Biol. Chem.* **259,** 3368–3374 Medline
7. Yap, L. L., Lin, M. T., Ouyang, H., Samoilova, R. I., Dikanov, S. A., and Gennis, R. B. (2010) The quinone-binding sites of the cytochrome *bo3* ubiquinol oxidase from *Escherichia coli*. *Biochim. Biophys. Acta* **1797,** 1924–1932 CrossRef Medline
8. Sena, F. V., Batista, A. P., Catarino, T., Brito, J. A., Archer, M., Viertler, M., Madl, T., Cabrita, E. J., and Pereira, M. M. (2015) Type-II NADH:quinone oxidoreductase from *Staphylococcus aureus* has two distinct binding sites and is rate limited by quinone reduction. *Mol. Microbiol.* **98,** 272–288 CrossRef Medline
9. Filkins, L. M., Graber, J. A., Olson, D. G., Dolben, E. L., Lynd, L. R., Bhuju, S., and O'Toole, G. A. (2015) Coculture of *Staphylococcus aureus* with *Pseudomonas aeruginosa* drives *S. aureus* towards fermentative metabolism and reduced viability in a cystic fibrosis model. *J. Bacteriol.* **197,** 2252–2264 CrossRef Medline
10. Hazan, R., Que, Y. A., Maura, D., Strobel, B., Majcherczyk, P. A., Hopper, L. R., Wilbur, D. J., Hreha, T. N., Barquera, B., and Rahme, L. G. (2016) Auto poisoning of the respiratory chain by a quorum-sensing-regulated molecule favors biofilm formation and antibiotic tolerance. *Curr. Biol.* **26,** 195–206 CrossRef Medline
11. Lépine, F., Déziel, E., Milot, S., and Rahme, L. G. (2003) A stable isotope dilution assay for the quantification of the *Pseudomonas* quinolone signal in *Pseudomonas aeruginosa* cultures. *Biochim. Biophys. Acta* **1622,** 36–41 CrossRef Medline
12. Ortori, C. A., Dubern, J.-F., Chhabra, S. R., Cámara, M., Hardie, K., Williams, P., and Barrett, D. A. (2011) Simultaneous quantitative profiling of *N*-acyl-L-homoserine lactone and 2-alkyl-4(1*H*)-quinolone families of quorum-sensing signaling molecules using LC-MS/MS. *Anal. Bioanal. Chem.* **399,** 839–850 CrossRef Medline
13. Stover, C. K., Pham, X. Q., Erwin, A. L., Mizoguchi, S. D., Warrener, P., Hickey, M. J., Brinkman, F. S., Hufnagle, W. O., Kowalik, D. J., Lagrou, M., Garber, R. L., Goltry, L., Tolentino, E., Westbrock-Wadman, S., Yuan, Y., *et al.* (2000) Complete genome sequence of *Pseudomonas aeruginosa* PAO1, an opportunistic pathogen. *Nature* **406,** 959–964 CrossRef Medline
14. Déziel, E., Lépine, F., Milot, S., He, J., Mindrinos, M. N., Tompkins, R. G., and Rahme, L. G. (2004) Analysis of *Pseudomonas aeruginosa* 4-hydroxy-2-alkylquinolines (HAQs) reveals a role for 4-hydroxy-2-heptylquinoline in cell-to-cell communication. *Proc. Natl. Acad. Sci. U.S.A.* **101,** 1339–1344 CrossRef Medline
15. Dulcey, C. E., Dekimpe, V., Fauvelle, D. A., Milot, S., Groleau, M. C., Doucet, N., Rahme, L. G., Lépine, F., and Déziel, E. (2013) The end of an old hypothesis: the *Pseudomonas* signaling molecules 4-hydroxy-2-alkylquinolines derive from fatty acids, not 3-ketofatty acids. *Chem. Biol.* **20,** 1481–1491 CrossRef Medline
16. Oke, M., Carter, L. G., Johnson, K. A., Liu, H., McMahon, S. A., Yan, X., Kerou, M., Weikart, N. D., Kadi, N., Sheikh, M. A., Schmelz, S., Dorward, M., Zawadzki, M., Cozens, C., Falconer, H., Powers, H., Overton, I. M., *et al.* (2010) The Scottish structural proteomics facility: targets, methods and outputs. *J. Struct. Funct. Genomics* **11,** 167–180 CrossRef Medline
17. D'Argenio, D. A., Calfee, M. W., Rainey, P. B., and Pesci, E. C. (2002) Autolysis and autoaggregation in *Pseudomonas aeruginosa* colony morphology mutants. *J. Bacteriol.* **184,** 6481–6489 CrossRef Medline
18. van Berkel, W. J., Kamerbeek, N. M., and Fraaije, M. W. (2006) Flavoprotein monooxygenases, a diverse class of oxidative biocatalysts. *J. Biotechnol.* **124,** 670–689 CrossRef Medline

19. van Pée, K. H., and Patallo, E. P. (2006) Flavin-dependent halogenases involved in secondary metabolism in bacteria. *Appl. Microbiol. Biotechnol.* **70,** 631–641 CrossRef Medline
20. Mascotti, M. L., Juri Ayub, M., Furnham, N., Thornton, J. M., and Laskowski, R. A. (2016) Chopping and changing: the evolution of the flavin-dependent monooxygenases. *J. Mol. Biol.* **428,** 3131–3146 CrossRef Medline
21. Husain, M., and Massey, V. (1979) Kinetic studies on the reaction of *p*-hydroxybenzoate hydroxylase. Agreement of steady state and rapid reaction data. *J. Biol. Chem.* **254,** 6657–6666 Medline
22. Massey, V. (1991) *A Simple Method for Determination of Redox Potentials, Flavins and Flavoproteins* (Curti, B., Zanetti, G., and Ronchi, S., eds) pp. 59–66, Walter de Gruyter, Berlin
23. Crozier-Reabe, K., and Moran, G. R. (2012) Form follows function: structural and catalytic variation in the class a flavoprotein monooxygenases. *Int. J. Mol. Sci.* **13,** 15601–15639 CrossRef Medline
24. Palfey, B. A., Ballou, D. P., and Massey, V. (1995) *Active Oxygen in Biochemistry*, pp. 37–83, Springer, Dordrecht, Netherlands
25. Einarsdottir, G. H., Stankovich, M. T., Powlowski, J., Ballou, D. P., and Massey, V. (1989) Regulation of oxidation-reduction potentials of anthranilate hydroxylase from *Trichosporon cutaneum* by substrate and effector binding. *Biochemistry* **28,** 4161–4168 CrossRef Medline
26. Williamson, G., Edmondson, D. E., and Müller, F. (1988) Oxidation-reduction potential studies on *p*-hydroxybenzoate hydroxylase from *Pseudomonas fluorescens*. *Biochim. Biophys. Acta* **953,** 258–262 CrossRef Medline
27. Huijbers, M. M., Montersino, S., Westphal, A. H., Tischler, D., and van Berkel, W. J. (2014) Flavin dependent monooxygenases. *Arch. Biochem. Biophys.* **544,** 2–17 CrossRef Medline
28. Hammer, P. E., Hill, D. S., Lam, S. T., Van Pée, K. H., and Ligon, J. M. (1997) Four genes from *Pseudomonas fluorescens* that encode the biosynthesis of pyrrolnitrin. *Appl. Environ. Microbiol.* **63,** 2147–2154 Medline
29. Galán, B., Díaz, E., Prieto, M. A., and García, J. L. (2000) Functional analysis of the small component of the 4-hydroxyphenylacetate 3-monooxygenase of *Escherichia coli* W: a prototype of a new flavin:NAD(P)H reductase subfamily. *J. Bacteriol.* **182,** 627–636 CrossRef Medline
30. Otto, K., Hofstetter, K., Röthlisberger, M., Witholt, B., and Schmid, A. (2004) Biochemical characterization of StyAB from *Pseudomonas* sp. strain VLB120 as a two-component flavin-diffusible monooxygenase. *J. Bacteriol.* **186,** 5292–5302 CrossRef Medline
31. Chakraborty, S., Ortiz-Maldonado, M., Entsch, B., and Ballou, D. P. (2010) Studies on the mechanism of *p*-hydroxyphenylacetate 3-hydroxylase from *Pseudomonas aeruginosa*: a system composed of a small flavin reductase and a large flavin-dependent oxygenase. *Biochemistry* **49,** 372–385 CrossRef Medline
32. Sucharitakul, J., Tinikul, R., and Chaiyen, P. (2014) Mechanisms of reduced flavin transfer in the two-component flavin-dependent monooxygenases. *Arch. Biochem. Biophys.* **555,** 33–46 Medline
33. Arunachalam, U., Massey, V., and Miller, S. M. (1994) Mechanism of *p*-hydroxyphenylacetate-3-hydroxylase. A two-protein enzyme. *J. Biol. Chem.* **269,** 150–155 Medline
34. Louie, T. M., Xie, X. S., and Xun, L. (2003) Coordinated production and utilization of $FADH_2$ by NAD(P)H–flavin oxidoreductase and 4-hydroxyphenylacetate 3-monooxygenase. *Biochemistry* **42,** 7509–7517 CrossRef Medline
35. Gibson, Q. H., and Hastings, J. W. (1962) The oxidation of reduced flavin mononucleotide by molecular oxygen. *Biochem. J.* **83,** 368–377 CrossRef Medline
36. Xun, L., and Sandvik, E. R. (2000) Characterization of 4-hydroxyphenylacetate 3-hydroxylase (HpaB) of *Escherichia coli* as a reduced flavin adenine dinucleotide-utilizing monooxygenase. *Appl. Environ. Microbiol.* **66,** 481–486 CrossRef Medline
37. Unversucht, S., Hollmann, F., Schmid, A., and van Pée, K. H. (2005) $FADH_2$-dependence of tryptophan 7-halogenase. *Adv. Synth. Catal.* **347,** 1163–1167 CrossRef
38. Buedenbender, S., Rachid, S., Müller, R., and Schulz, G. E. (2009) Structure and action of the myxobacterial chondrochloren halogenase CndH: A new variant of FAD-dependent halogenases. *J. Mol. Biol.* **385,** 520–530 CrossRef Medline
39. Tu, S. C. (2001) Reduced flavin: donor and acceptor enzymes and mechanisms of channeling. *Antioxid. Redox Signal.* **3,** 881–897 CrossRef Medline
40. Green, L. K., Storey, M. A., Williams, E. M., Patterson, A. V., Smaill, J. B., Copp, J. N., and Ackerley, D. F. (2013) The flavin reductase MsuE is a novel nitroreductase that can efficiently activate two promising next-generation prodrugs for gene-directed enzyme prodrug therapy. *Cancers* **5,** 985–997 CrossRef Medline
41. Palmer, G. C., Jorth, P. A., and Whiteley, M. (2013) The role of two *Pseudomonas aeruginosa* anthranilate synthases in tryptophan and quorum signal production. *Microbiology* **159,** 959–969 CrossRef Medline
42. Drees, S. L., Li, C., Prasetya, F., Saleem, M., Dreveny, I., Williams, P., Hennecke, U., Emsley, J., and Fetzner, S. (2016) PqsBC, a condensing enzyme in the biosynthesis of the *Pseudomonas aeruginosa* quinolone signal: crystal structure, inhibition, and reaction mechanism. *J. Biol. Chem.* **291,** 6610–6624 CrossRef Medline
43. Huntress, E. H., Lesslie, T. E., and Hearon, W. M. (1956) A new route to 1-aryl pyrroles. *J. Am. Chem. Soc.* **78,** 419–423 CrossRef
44. Kamm, O. (2003) in *Organic Syntheses*, pp. 57–57, John Wiley & Sons, Inc., Hoboken, NJ CrossRef
45. Millen, M. H., and Waters, W. A. (1971) Reactions between aromatic nitro-compounds and hydroxylamines in alkaline solution. Part II. Product studies. *J. Chem. Soc. B Phys. Org.* **1971,** 2398–2400 CrossRef
46. Kim, Y. H., Song, W. S., Go, H., Cha, C. J., Lee, C., Yu, M. H., Lau, P. C., and Lee, K. (2013) 2-Nitrobenzoate 2-nitroreductase (NbaA) switches its substrate specificity from 2-nitrobenzoic acid to 2,4-dinitrobenzoic acid under oxidizing conditions. *J. Bacteriol.* **195,** 180–192 CrossRef Medline
47. Schnell, S., and Mendoza, C. (2000) Enzyme kinetics of multiple alternative substrates. *J. Math. Chem.* **27,** 155–170 CrossRef
48. Schäuble, S., Stavrum, A. K., Puntervoll, P., Schuster, S., and Heiland, I. (2013) Effect of substrate competition in kinetic models of metabolic networks. *FEBS Lett.* **587,** 2818–2824 CrossRef Medline
49. Cárdenas, M. L. (2001) The competition plot: a kinetic method to assess whether an enzyme that catalyzes multiple reactions does so at a unique site. *Methods* **24,** 175–180 CrossRef Medline
50. Pocklington, T., and Jeffery, J. (1969) Competition of two substrates for a single enzyme. A simple kinetic theorem exemplified by a hydroxy steroid dehydrogenase reaction. *Biochem. J.* **112,** 331–334 CrossRef Medline
51. Beland, F. A., and Kadlubar, F. F. (1985) Formation and persistence of arylamine DNA adducts *in vivo*. *Environ. Health Perspect.* **62,** 19–30 CrossRef Medline
52. Humphreys, W. G., Kadlubar, F. F., and Guengerich, F. P. (1992) Mechanism of C8 alkylation of guanine residues by activated arylamines: evidence for initial adduct formation at the N7 position. *Proc. Natl. Acad. Sci. U.S.A.* **89,** 8278–8282 CrossRef Medline
53. Kriek, E. (1974) Carcinogenesis by aromatic amines. *Biochim. Biophys. Acta* **355,** 177–203 Medline
54. Verna, L., Whysner, J., and Williams, G. M. (1996) 2-Acetylaminofluorene mechanistic data and risk assessment: DNA reactivity, enhanced cell proliferation and tumor initiation. *Pharmacol. Ther.* **71,** 83–105 CrossRef Medline
55. Borenfreund, E., Krim, M., and Bendich, A. (1964) Chromosomal aberrations induced by hyponitrite and hydroxylamine derivatives. *J. Natl. Cancer Inst.* **32,** 667–679 Medline
56. Eppink, M. H., Schreuder, H. A., and van Berkel, W. J. (1998) Interdomain binding of NADPH in *p*-Hydroxybenzoate hydroxylase as suggested by kinetic, crystallographic and modeling studies of histidine 162 and arginine 269 variants. *J. Biol. Chem.* **273,** 21031–21039 CrossRef Medline
57. Eppink, M. H., Overkamp, K. M., Schreuder, H. A., and Van Berkel, W. J. (1999) Switch of coenzyme specificity of *p*-hydroxybenzoate hydroxylase. *J. Mol. Biol.* **292,** 87–96 CrossRef Medline
58. Wang, J., Ortiz-Maldonado, M., Entsch, B., Massey, V., Ballou, D., and Gatti, D. L. (2002) Protein and ligand dynamics in 4-hydroxybenzoate hydroxylase. *Proc. Natl. Acad. Sci. U.S.A.* **99,** 608–613 CrossRef Medline

59. Eppink, M. H., Bunthol, C., Schreuder, H. A., and van Berkel, W. J. (1999) Phe^{161} and Arg^{166} variants of *p*-hydroxybenzoate hydroxylase. *FEBS Lett.* **443,** 251–255 CrossRef Medline
60. Eppink, M. H., Schreuder, H. A., and van Berkel, W. J. (1998) Lys42 and Ser42 variants of *p*-hydroxybenzoate hydroxylase from *Pseudomonas fluorescens* reveal that Arg42 is essential for NADPH binding. *Eur. J. Biochem.* **253,** 194–201 CrossRef Medline
61. van Berkel, W. J., Müller, F., Jekel, P. A., Weijer, W. J., Schreuder, H. A., and Wierenga, R. K. (1988) Chemical modification of tyrosine-38 in *p*-hydroxybenzoate hydroxylase from *Pseudomonas fluorescens* by 5′-*p*-fluorosulfonylbenzoyladenosine: a probe for the elucidation of the NADPH binding site? Involvement in catalysis, assignment in sequence and fitting. *Eur. J. Biochem.* **176,** 449–459 CrossRef Medline
62. Bendová, L., Jurecka, P., Hobza, P., and Vondrásek, J. (2007) Model of peptide bond-aromatic ring interaction: correlated ab initio quantum chemical study. *J. Phys. Chem. B* **111,** 9975–9979 CrossRef Medline
63. Schreuder, H. A., Mattevi, A., Obmolova, G., Kalk, K. H., Hol, W. G., van der Bolt, F. J., and van Berkel, W. J. (1994) Crystal structures of wild-type *p*-hydroxybenzoate hydroxylase complexed with 4-aminobenzoate, 2,4-dihydroxybenzoate, and 2-hydroxy-4-aminobenzoate and of the Tyr222Ala mutant complexed with 2-hydroxy-4-aminobenzoate. evidence for a proton channel and a new binding mode of the flavin. *Biochemistry* **33,** 10161–10170 CrossRef Medline
64. Palfey, B. A., Ballou, D. P., and Massey, V. (1997) Flavin conformational changes in the catalytic cycle of *p*-hydroxybenzoate hydroxylase substituted with 6-azido- and 6-aminoflavin adenine dinucleotide. *Biochemistry* **36,** 15713–15723 Medline
65. Wimpenny, J. W., and Firth, A. (1972) Levels of nicotinamide adenine dinucleotide and reduced nicotinamide adenine dinucleotide in facultative bacteria and the effect of oxygen. *J. Bacteriol.* **111,** 24–32 Medline
66. Drees, S. L., and Fetzner, S. (2015) PqsE of *Pseudomonas aeruginosa* acts as pathway-specific thioesterase in the biosynthesis of alkylquinolone signaling molecules. *Chem. Biol.* **22,** 611–618 CrossRef Medline
67. Needham, E. R., and Perkin, W. H. (1904) XVI.—*o*-Nitrobenzoylacetic acid. *J. Chem. Soc. Trans.* **85,** 148–155 CrossRef
68. Schöpf, C., Koepke, G., Kowald, B., Schülde, F., and Wunderlich, D. (1956) Darstellung und eigenschaften der *o*-formamino- und der *o*-amino-benzoylessigsäure, zweier zellmöglicher abbauprodukte des tryptophans und heteroauxins. *Chem. Ber.* **89,** 2877–2886 CrossRef
69. Sicker, D., and Mann, G. (1988) Synthesis of ethyl ortho-substituted benzoylacetates and investigation of the influence of ortho-substituents on keto-enol tautomerism and MS fragmentation behaviour. *Collect. Czechoslov. Chem. Commun.* **53,** 839–850 CrossRef
70. Zor, T., and Selinger, Z. (1996) Linearization of the Bradford protein assay increases its sensitivity: theoretical and experimental studies. *Anal. Biochem.* **236,** 302–308 CrossRef Medline
71. Whitby, L. G. (1953) A new method for preparing flavin-adenine dinucleotide. *Biochem. J.* **54,** 437–442 CrossRef Medline
72. Ho, S. N., Hunt, H. D., Horton, R. M., Pullen, J. K., and Pease, L. R. (1989) Site-directed mutagenesis by overlap extension using the polymerase chain reaction. *Gene* **77,** 51–59 CrossRef Medline
73. Jagmann, N., Brachvogel, H.-P., and Philipp, B. (2010) Parasitic growth of *Pseudomonas aeruginosa* in co-culture with the chitinolytic bacterium *Aeromonas hydrophila*. *Environ. Microbiol.* **12,** 1787–1802 CrossRef Medline
74. Emsley, P., Lohkamp, B., Scott, W. G., and Cowtan, K. (2010) Features and development of Coot. *Acta Crystallogr. D Biol. Crystallogr.* **66,** 486–501 CrossRef Medline
75. Winn, M. D., Ballard, C. C., Cowtan, K. D., Dodson, E. J., Emsley, P., Evans, P. R., Keegan, R. M., Krissinel, E. B., Leslie, A. G., McCoy, A., McNicholas, S. J., Murshudov, G. N., Pannu, N. S., Potterton, E. A., Powell, H. R., *et al.* (2011) Overview of the CCP4 suite and current developments. *Acta Crystallogr. D Biol. Crystallogr.* **67,** 235–242 CrossRef Medline
76. Murshudov, G. N., Vagin, A. A., and Dodson, E. J. (1997) Refinement of macromolecular structures by the maximum-likelihood method. *Acta Crystallogr. D Biol. Crystallogr.* **53,** 240–255 CrossRef Medline
77. Adams, P. D., Afonine, P. V., Bunkóczi, G., Chen, V. B., Davis, I. W., Echols, N., Headd, J. J., Hung, L.-W., Kapral, G. J., Grosse-Kunstleve, R. W., McCoy, A. J., Moriarty, N. W., Oeffner, R., Read, R. J., Richardson, D. C., *et al.* (2010) PHENIX: a comprehensive Python-based system for macromolecular structure solution. *Acta Crystallogr. D Biol. Crystallogr.* **66,** 213–221 CrossRef Medline
78. Terwilliger, T. C., Grosse-Kunstleve, R. W., Afonine, P. V., Moriarty, N. W., Zwart, P. H., Hung, L. W., Read, R. J., and Adams, P. D. (2008) Iterative model building, structure refinement and density modification with the PHENIX AutoBuild wizard. *Acta Crystallogr. D Biol. Crystallogr.* **64,** 61–69 CrossRef Medline
79. Coleman, J. P., Hudson, L. L., McKnight, S. L., Farrow, J. M., 3rd., Calfee, M. W., Lindsey, C. A., and Pesci, E. C. (2008) *Pseudomonas aeruginosa* PqsA is an anthranilate-coenzyme A ligase. *J. Bacteriol.* **190,** 1247–1255 CrossRef Medline
80. Zhang, Y.-M., Frank, M. W., Zhu, K., Mayasundari, A., and Rock, C. O. (2008) PqsD is responsible for the synthesis of 2,4-dihydroxyquinoline, an extracellular metabolite produced by *Pseudomonas aeruginosa*. *J. Biol. Chem.* **283,** 28788–28794 CrossRef Medline